Engineering Fracture Mechanics xxx (2011) xxx–xxx

Contents lists available at SciVerse ScienceDirect

Engineering Fracture Mechanics

journal homepage: www.elsevier.com/locate/engfracmech

Effect of fracture tunneling in DWT Tests

E. Marotta, M. Minotti, P. Salvini *

Department of Mechanical Engineering, University of Rome "Tor Vergata", Via del Politecnico, 1, 00133 Roma, Italy

ARTICLE INFO

Article history:
Available online xxxx

Keywords:
Fracture tunneling
Fracture propagation
DWT Tests

ABSTRACT

The work deals with the effective shape of the fracture during a Drop Weight Tear Test (DWT). An inexpensive technique, able to determine the geometrical shape of the fracture, is discussed and presented. The technique is capable to perform reliable measurements and offers a mathematical description of the fracture profile. In few words, the fracture tunneling measurement and its correlated effects are the objectives of this work. The technique is based on a copy of the fracture by a silicone mold, followed by a digital analysis of the tomographic images. The attention is finally focused on two different steels used in inshore gas piping. The tunneling measurement is exploited in a finite element simulation of the fracture propagation, thus opening the opportunity to update the kinematic models applied for Crack Tip Opening Angle assessment.

1. Introduction

In the analysis of integrity and reliability of buried pipelines, a fundamental issue concerns the running behavior of a crack, when for some reason, it appears on the pipe. As a matter of fact, after starting, the crack might propagate at an almost stable speed or might gradually decelerate until arrest, according to the general characteristics and ductile properties of the steel used [1,2].

With the aim to identify the resistance force that a pipeline is able to oppose the driving force, given by the pressurized gas, instrumented Drop Weight Tear Tests (DWTs) are performed on SENB-shaped specimens [3–5]. The output of these tests are the measurement of the energy lost during the steady state propagation of the crack. Through energy computation, performed with the application of a two ligament method [6,7] or a single test method [8,9], the ductile characteristics of the steel can be deduced. The tests are conducted in full thickness on a flattened specimen extracted from the pipe, so that the results are not suitable to characterize the material, but the pipeline, instead.

The performed tests are however far from the effective conditions of a crack, running on a pipeline, for several reasons [10]. One aspect regards the actual shape of the fracture front in the thickness, which can remarkably affect the results deduced through the methods previously mentioned. In other words, the crack appearance on the surface does not give evidence of the effective crack front inside the specimen.

In Ref. [11] it is claimed that the crack inner profile, when stable propagation occurs, presents an internal development which is self-similar. The profile of the fracture shifts in the direction of propagation with only minor modifications of its shape.

Most of the methods aimed to connect the DWT Tests with the Full Scale Burst Tests make use of the Crack Tip Opening Angle inference. According to all these models, the three dimensional development of the fracture is averaged on the thickness. Thus, the crack tip is identified by a unique representative value, regardless of the specimen thickness. Following this

* Corresponding author.
E-mail address: salvini@uniroma2.it (P. Salvini).

0013-7944/$ - see front matter © 2011 Elsevier Ltd. All rights reserved.
doi:10.1016/j.engfracmech.2011.09.003

simplified assumption, the residual ligament determination is straightforward, and a direct kinematical method for the fracture progression can be applied [12].

After the direct exam of the fracture profiles, it is well known that the fracture front in the thickness, even if self-similar, develops in a nontrivial way [13]. With a particular emphasis on ductile fracture propagation, crack tunneling can be evidenced [14], interesting an extension that is comparable or even greater than the specimen thickness itself.

In previous works, using subsequent frames of images taken during a DWT Test [15,16] where moving and fixed targets are identified, the following automatic evaluations have been performed: opening angle of the two halves of the specimen; progression of the crack tip at the specimen surface; critical CTOA value according to model [17]; actual Center of Instantaneous Rotation of the two specimen halves during bending. The movements of the CIR deduced by image processing partially confirm the application of the analytical model described in [12]. However, it is observed a value of the rotational parameter called r^* (dimensionless ratio that identifies the CIR location by respect to the initial ligament), considerably higher than the previously well-established values, relative to non-high strength steels [18,19]. This scattering can be partially charged to the presence of an internal crack front which is non-orthogonal to the specimen surface (tunneling). Some researchers already remarked the higher values of r^* for high strength steels [20], but they charged this scatter to the hardening effect, thus forgetting the tunneling one, which, as it is claimed in the present work, plays a very important role.

A mathematical representation of a casting of the crack front region would be helpful in determining an equivalent position for the crack front, and could modify the scatter on r^* values. Furthermore, it is possible to realize a more realistic 3-D mesh for Finite Element computations, taking advantage of an updated value of the ligament, so that the model [12] can be applied in a more reliable form.

The present analysis is performed on two different pipeline steels, classified as X100 and X60, according to the API standards, with different thicknesses. The first one is a high strength 21 mm thick steel, while the second one is a lower strength steel, presenting a thickness of 12 mm.

2. The technique to detect the crack profile

In a DWT Test the specimen is broken by means of the energy released by an impact hammer. Generally, the specimen is fully broken. The high test speed makes measurement difficult, but measurement techniques able to monitor the crack conformation and progression during the event are nowadays available and have already been used for DWTT [21]. However, they still do not allow the digital resolution here used (12 Mega Pixel), requested to detect the effective movement, that is used in the kinematical analysis of the two forming halves of the DWTT specimen, as explained in [22]. In the above mentioned application, considering the whole image field necessary for DWTT analysis, the conversion coefficient mm/pixel is around 0.05.

Nevertheless, it is expected that this capability will be soon available, given the rapid developments, both in technical and in economical terms, of the digital optical devices.

With this aim, in previous works [15,16] a new three point bending device has been developed, which is capable to reconstruct the static tests in detail. The proposed device is also able to perform tests where the impact hammer has a continuous moving forward, even if its speed is much lower than that experienced in a DWTT.

In the static experiment it is possible to stop the test when the crack lies inside the region of stable propagation [23,24] characterized by a stable CTOA value. From this uncompleted test it is possible to attempt the analysis of the crack conformation.

The technique consists in the realization of a mold of the fracture, thus allowing the analysis of the crack shape. The mold is formed starting from a liquid silicone resin, with the addition of its catalyst to promote curing. This silicone resin has an optimal elasticity and flexibility, with good non-stick characteristics. In its initial liquid state the low viscosity allows to fill the entire cavity opened by the fracture. During the casting, it is necessary to mind the formation of air pockets, which would compromise the fidelity of the copy. This last requirement made it necessary to remove the specimen from the machine before casting.

The extraction of the cast is possible after complete solidification, but the only way to achieve it, without any cast damage, is to proceed with the fracture until the final separation of the specimen. Therefore, it is necessary to reallocate the specimen on the supports after the silicone curing, and complete the test. Only in this way one obtains that the silicone copy does not present any rupture close to the crack tip. Within the obtained cast, it is easy to evidence the necking, the surface aspect and the tunneling formed inside the thickness (Fig. 1).

The digital description of the surface of the fracture needs, to be completed, the application of a reverse engineering technique [25], such as laser scanning. However, this is not so easy, since the surface presents many irregularities, and the quasi fractal surface causes light beam scattering. Here, to get the digital representation of the fracture surface, a procedure that is equivalent to a tomographic or stratigraphic technique is adopted. This procedure does not rely to a standard, but allowed a good reliability level accompanied with the use of simple instrumentation. The tomographic technique allows the representation of solids through the overlap of stratified two-dimensional images. The equipment used is readily available and is composed of: a 12 Mega Pixels digital camera, a black colored liquid with low surface tension, a reference object of known geometry (pyramidal), two graded containers communicating through a rubber tube driven by a flow control valve. The cast and the reference object are contained in a box where a diffusive illumination is applied. The cast is fixed to the bottom of

Please cite this article in press as: Marotta E et al. Effect of fracture tunneling in DWT Tests. Engng Fract Mech (2011), doi:10.1016/j.engfracmech.2011.09.003

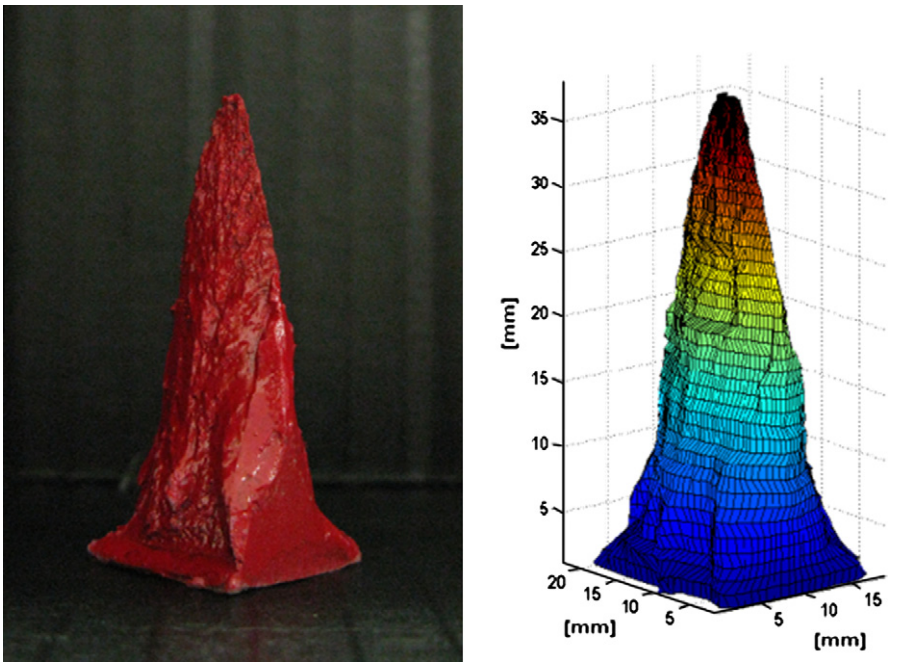

Fig. 1. Silicone cast of the inner fracture and its digital model.

one of the containers while the other is placed at a higher height, in order to allow the flow from the second to the first container (see Fig. 2). The liquid transfer, step by step, is governed through a valve. At each step a picture is taken, until the immersion of the cast is complete. The level of the liquid creates a reference plane, bordered by the emerging profile. The level is increased through the valve 1 mm at a time; thus the stratigraphy is characterized by the same step. The frames are taken with a low depth of focus (around 150 mm) with the *macro-function* activated. The focalization is continuously updated so that it is tuned to the effective level of the liquid where the profile of the cast is identified. The liquid used contains a percentage of surfactant in order to reduce the value of its surface tension. It is colored black to allow for a good

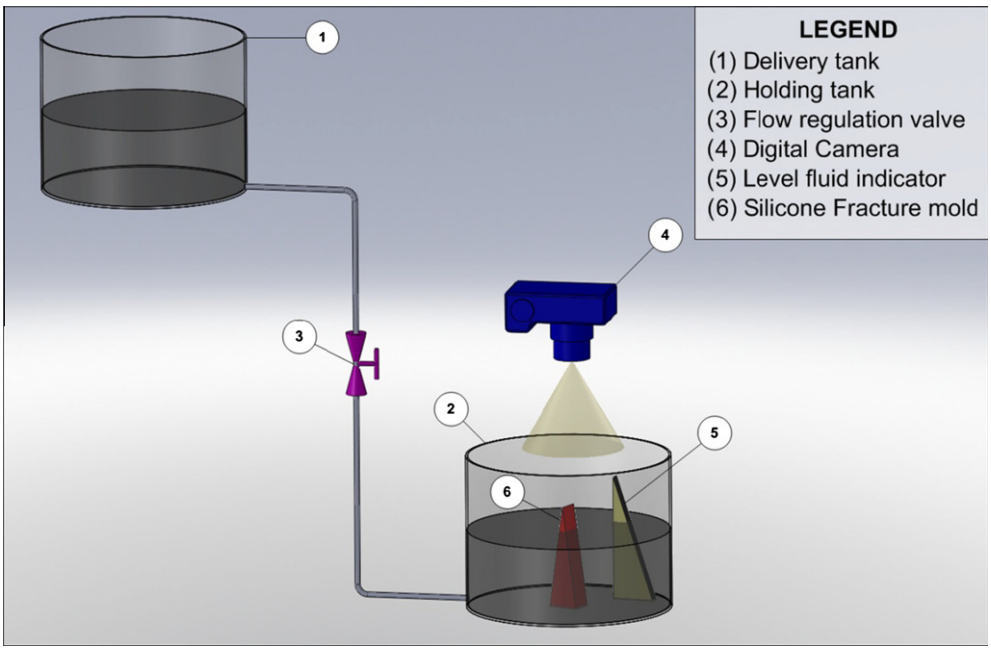

Fig. 2. Experimental layout for stratigraphy.

Please cite this article in press as: Marotta E et al. Effect of fracture tunneling in DWT Tests. Engng Fract Mech (2011), doi:10.1016/j.engfracmech.2011.09.003

contrast with the specimen, which in turn is painted red. All the collected pictures are then processed by a code written in the MatLab® environment that allows the virtual representation.

The presence of a reference object of known shape and dimensions (in this case a truncated pyramid) allows a rapid and direct knowledge of both the conversion mm/pixel (which can vary with the fine adjustment of the optical focus) and the actual level of the surface. This last is determined by the amount of the emerging pyramid, whose diagonal measurement is a check to control the imprecision introduced by the maneuvering of the valve. The measurement on the pyramid is affected by the partial surge of the liquid on the bordering solid (meniscus) that is also present at the cast border. Thus, the inaccuracies introduced by the meniscus are minimized.

Different liquids, with lower surface tension have been tested, but they are generally characterized by a low volatility. After some comparison tests, the conclusion is that their benefits do not justify their use.

3. Digitalization of the crack profile

The profile detected by subsequent images, digitally acquired, has to be numerically manipulated to accurately identify its border.

However, due to the continuous change in the focalization, it is necessary to compute, for any picture, both the effective conversion pixel/mm and the effective level of the liquid surface. To these purposes, the pyramid is truncated at its top, so that it provides both the conversion parameter through the measurement of the dimension of the top, and the liquid level through its edge acquisition (Fig. 3).

Two important aspects, introducing systematic errors, must be pointed out when managing photographic images: parallax effect and lens distortion. The first one can be easily corrected, knowing the distance between the focalization plane and the center of the focus, through simple trigonometric equations. Here the problem is very trivial since the object (fluid surface) keeps everywhere the same orthogonal distance from the focus. Due to the image field dimension, the expected error, if not properly corrected, reaches less than 3‰.

The second aspect, lens distortion, is related to the effective optics used and it requires suitable experiments. This imperfection can be emphasized by the use of macro or wide-angle lens. In Fig. 4 it is shown the distortion revealed by the camera used, with the macro-function activated, in the same focalization conditions adopted for the cast measurement.

A picture of a grid of circles is taken. Each circle is evidenced through its centroid, whose position differs from the red grid intersection that provides the ideal location of the centroid. The error shift, as expected, is grater away from the optical center (see e.g. the marker in the upper left or lower-right).

Referring to the technique described in [26], a model based on coefficients governing the tangential and radial distortions has been introduced:

$$u' = u + k_1 \cdot u \cdot (u^2 + v^2) + p_1 \cdot (3u^2 + v^2) + 2 \cdot u \cdot v \cdot p_2 \tag{1}$$

$$v' = v + k_1 \cdot v \cdot (u^2 + v^2) + 2 \cdot u \cdot v \cdot p_1 + p_2 \cdot (u^2 + 3v^2) \tag{2}$$

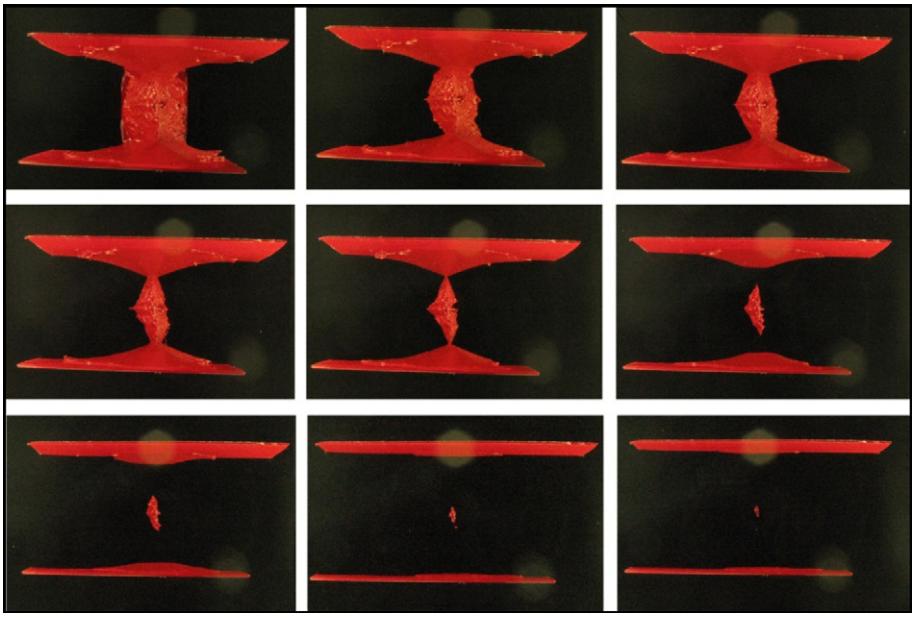

Fig. 3. Extract of the picture sequence for some liquid surface height.

Please cite this article in press as: Marotta E et al. Effect of fracture tunneling in DWT Tests. Engng Fract Mech (2011), doi:10.1016/j.engfracmech.2011.09.003

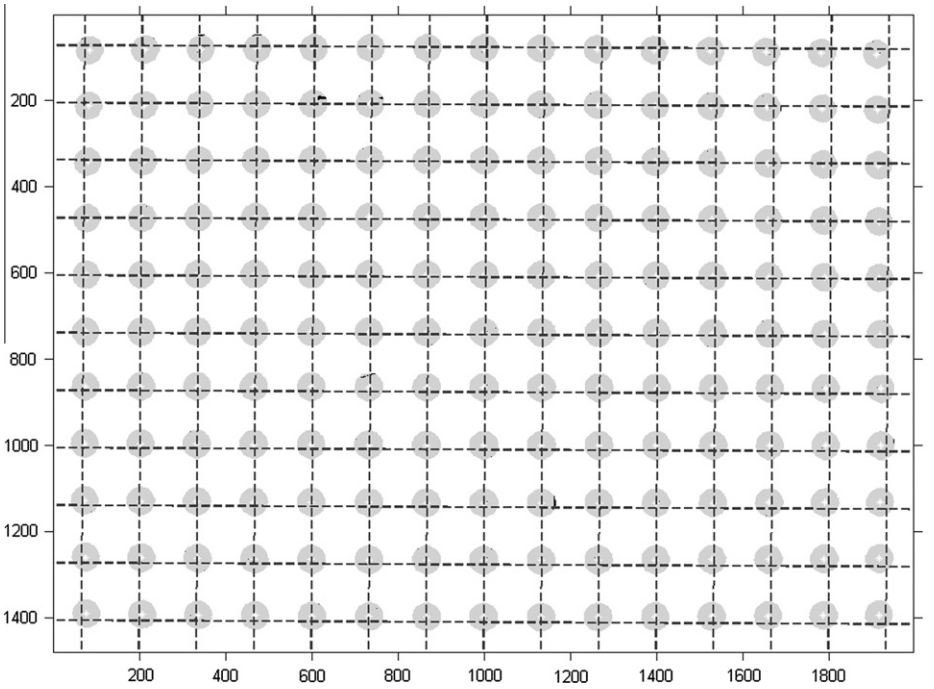

Fig. 4. Effect of the optical distortion. The dashed grid represents the correct circle location.

Table 1
Parameters optimized for distortion correction.

Parameter	k_1 Radial	p_1 Tangential x	p_2 Tangential y
Value	7.2612×10^{-9}	2.4449×10^{-6}	1.1076×10^{-6}

A reference system, based on two coordinates u and v, whose origin is in the center of the image, allows to describe the non-distorted coordinates u' and v', by means of the correction parameters k_1, p_1 and p_2. The first parameter acts in the radial direction, the remaining two in the tangential direction.

The correction coefficients are computed through the minimization of an objective function that accounts the shifts measured from the distorted grid and the ideal one. After some digital filtering, the grid is composed of gray circles on a white background.

Considering the camera used in this research, the digital resolution (2100×1200 pixels) and the focalization adopted while acquiring the images, the maximum distortions expected is 11.87 pixels in the vertical direction and 21.51 in the horizontal one. However, it should be noted that the images were processed only in a partial frame consisting of 600×600 pixels. Thus, the maximal distortion expected reduces to 1.5 pixels, which is close to 5‰ of the maximum distance from the optical center.

In conclusion, one can definitely say that the systematic errors introduced are negligible in the approximation requested by inner fracture measurement.

Nevertheless, at each taken picture, the distortion introduced can be minimized through the correction parameter given in Table 1.

It is useless to reach a better approximation, since the measured feature (crack tunneling) cannot be replicated with a higher similarity than the measuring reliability reached; in other words, one does not have any benefit to seek higher precisions than the intrinsic limit associated with the test data, which provide profiles always different at any repetition of the tests.

4. Comparison of the two examined steels

The resin casts and their 3-D digital representation have been performed on two specimens, different for material and thickness. The casts are extracted from interrupted tests, applied on SENB-like specimens. The first group of specimens are made of steel API X100, 21 mm thick, the second one are made of a steel API X60, 12 mm thick.

Please cite this article in press as: Marotta E et al. Effect of fracture tunneling in DWT Tests. Engng Fract Mech (2011), doi:10.1016/j.engfracmech.2011.09.003

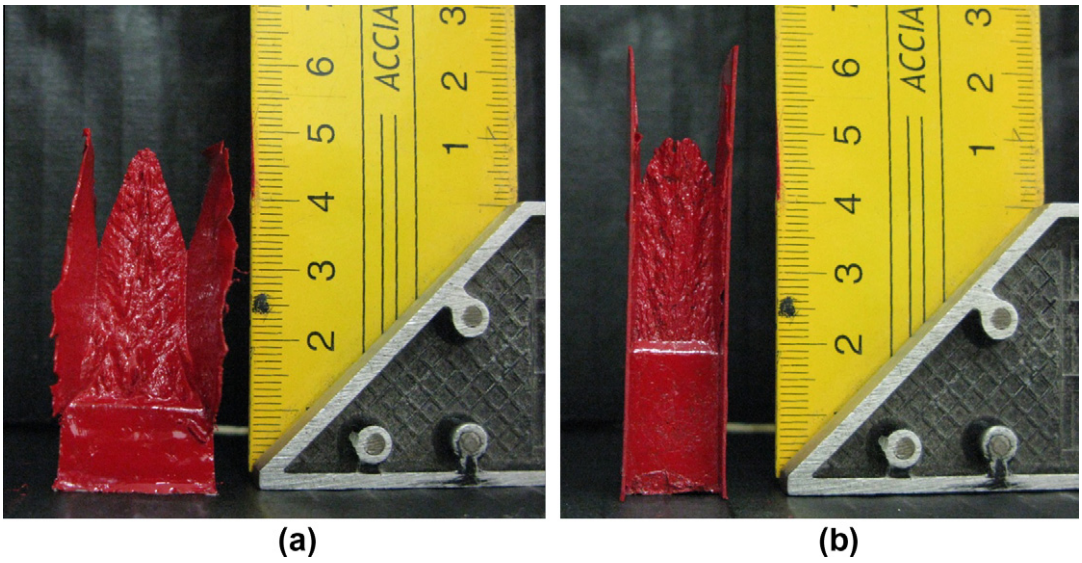

Fig. 5. Silicone casts for the (a) X100 21 mm thick specimens and (b) X60 12 mm thick.

The method used to evaluate the critical CTOA makes no difference for the two groups. Therefore, it is expected to verify a similar behavior through thickness, see Fig. 5.

Fig. 6 shows the digital reconstructions of the casts for the two materials. Contrary to what is expected there are evident differences in the aspects of the two tunneling shapes. The first presents a much greater extension in the sense of depth by comparison to the second one. Another important aspect regards the amount of necking, much more evident for the first material, even if it is characterized by a wider thickness. The necking is close to 35% for the X100 steel and 16% for the X60.

With the aim to have an insight of the tunneling (and CTOA) on different specimen depths, sections of the digital fracture are performed with different orthogonal planes. The first plane considered is in the middle of the specimen; the other planes

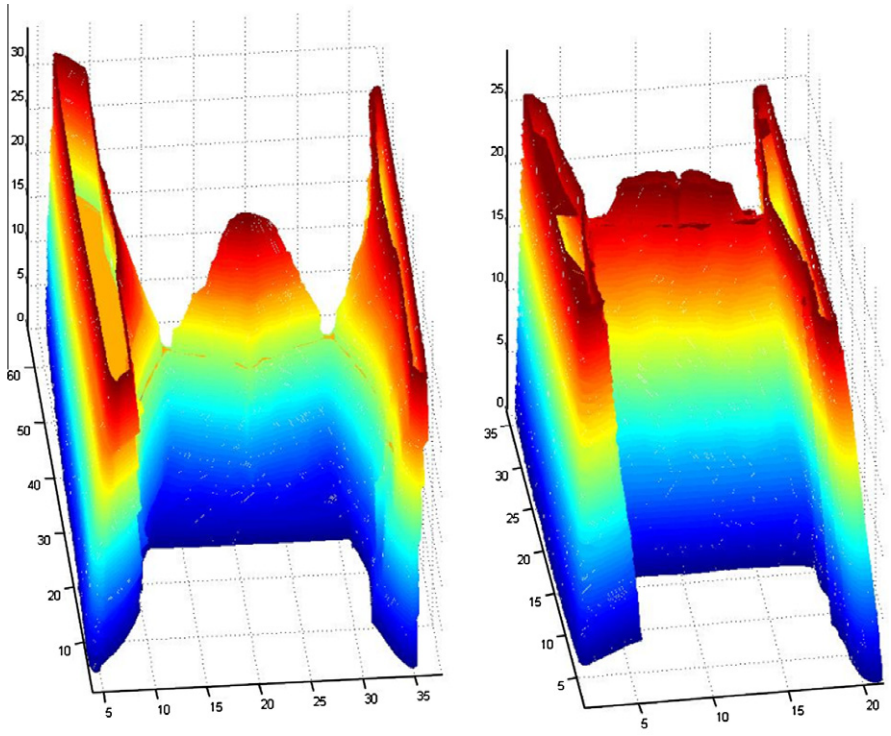

Fig. 6. Digital model of the fracture for the X100 – 21 mm thick and X60 – 12 mm thick.

Please cite this article in press as: Marotta E et al. Effect of fracture tunneling in DWT Tests. Engng Fract Mech (2011), doi:10.1016/j.engfracmech.2011.09.003

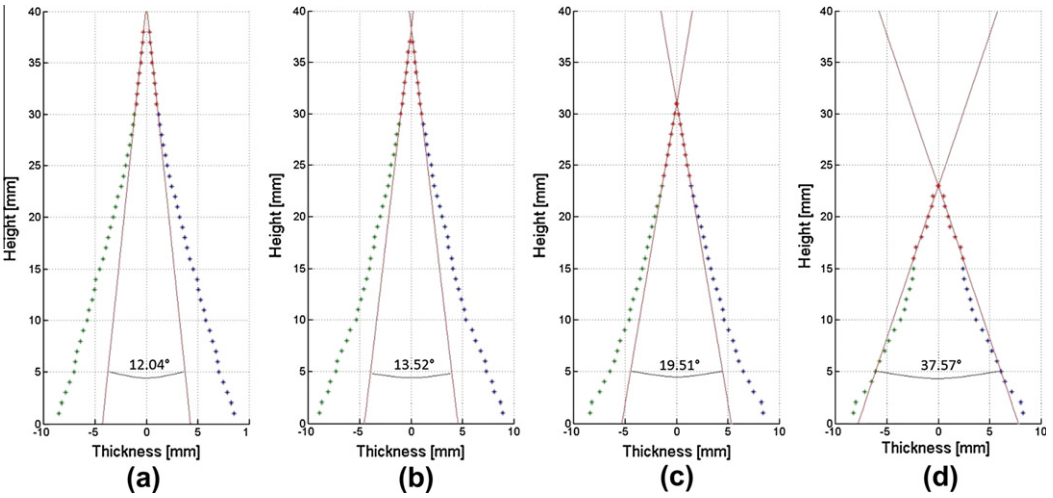

Fig. 7. Projections of the fracture profile of X100 steel by planes distinct from middle plane: (a) 0 mm (b) 2.25 mm (c) 4.5 mm (d) 6.75 mm.

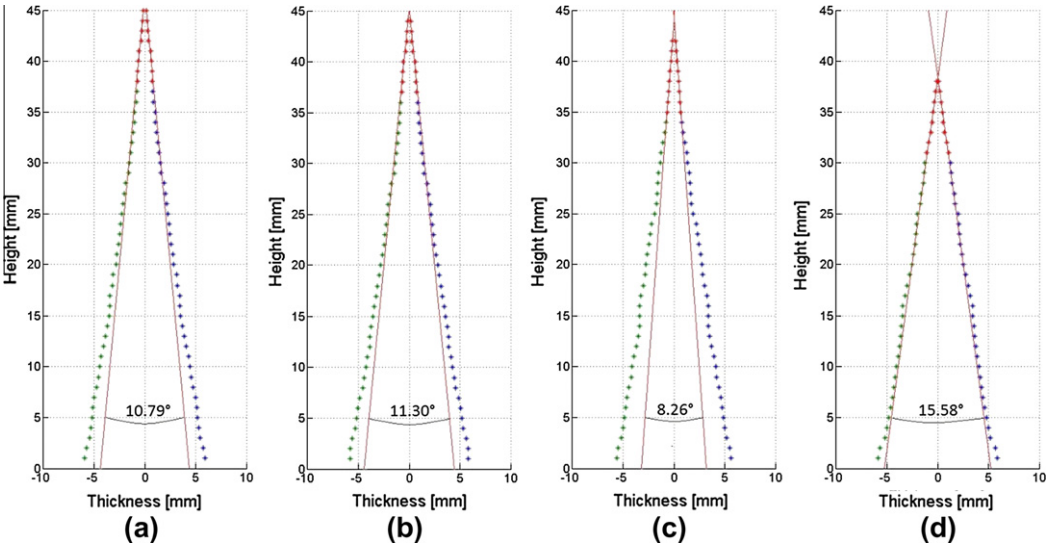

Fig. 8. Projections of the fracture profile of X60 steel by planes distinct from middle plane: (a) 0 mm (b) 2.25 mm (c) 4.5 mm (d) 6.75 mm.

are shifted from this middle plane of a fixed quantity, indicated in the captions of Figs. 7 and 8. The CTOA angles come from a fitting extended on the closer eight points.

The lines represent the tangents to these points. One can see that this angle remains fairly constant for the X60-12 mm Fig. 8, while in the case of X100-21 mm it varies more significantly. In the projection plane (d) of Fig. 7, where it reaches the highest value, it corresponds to the angle emerging from the sample. This measured value is in close agreement with the measurements taken by the picture of the specimen under tests, as shown in [15].

Previous Figs. 7 and 8 were made symmetric before their representation, by respect to the middle plane of fracture. This was done in order to evidence the nominal profiles. The benefit is appreciable by the comparison of the two profiles, measured and made symmetric, shown in Fig. 9. Partial inclusions or extrusions in the profiles do not alter the nominal crack shape, if appropriately corrected.

The measured CTOA values, in the direct comparison of the two steels, make it evident that the X100 presents an important deviation of the values from the core to the surface. The surface angle is particularly high, in accordance with the optical measurements, but it is much lower than the CTOA angle measured inside the specimen thickness. Another important consideration concerns the location of the crack tip, inside the specimen thickness. The difference between the inner location of the tip and its outer location reaches 81.0% of the thickness for the X100, but only 37.5% for the X60.

These last values indicate that the appearance of the crack in the surface of high strength materials gives only a very approximate location of the crack inside the specimen.

Please cite this article in press as: Marotta E et al. Effect of fracture tunneling in DWT Tests. Engng Fract Mech (2011), doi:10.1016/j.engfracmech.2011.09.003

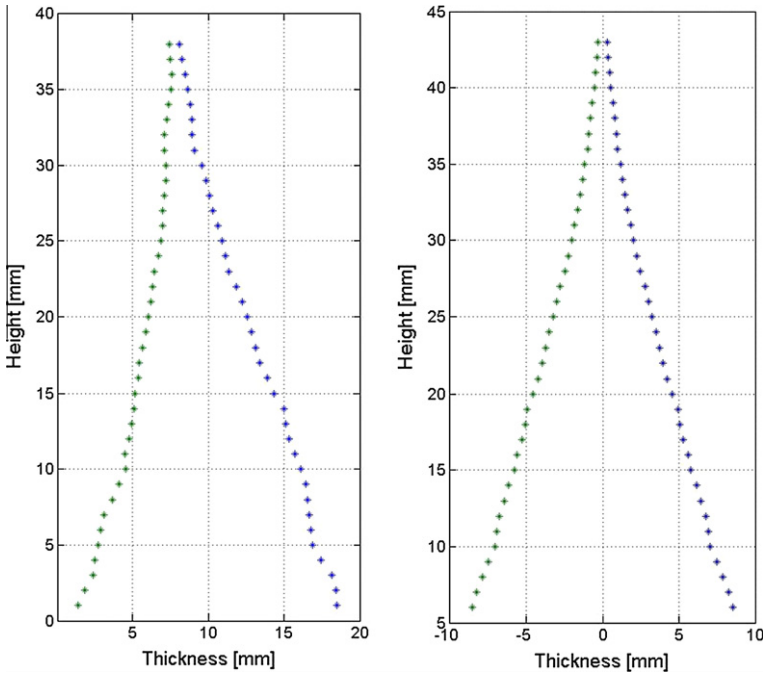

Fig. 9. Comparison of crack profile before and after the imposition of symmetry.

This discrepancy has an important issue in the CTOA measurements derived by DWT Tests. If the fracture tip, inside the specimen thickness, extends considerably forwards by respect to surface appearance, it results that the stress considerably reduces because of the linear decreasing nominal stress value applied by bending. This is completely missing in the r^* evaluation, whose value is essential for the critical conditions assessed during propagation in the DWTT (in the present case the critical CTOA). As a matter of fact, the r^* enters directly in the energy models used to compute the CTOA [8,12].

In a pipe, subjected to crack propagation, the nominal stress ahead the crack tip keeps almost stationary so that the tunneling effect is not so critical and the exact crack tip positioning is poorly influent.

Some considerations connected to this phenomenon are discussed by some authors [8,24], who claims that the r^* accounted when dealing with high strength steels should be properly increased. At which amount this increase should be attributed to material characteristic if not to crack tunneling remains a subject still under investigation.

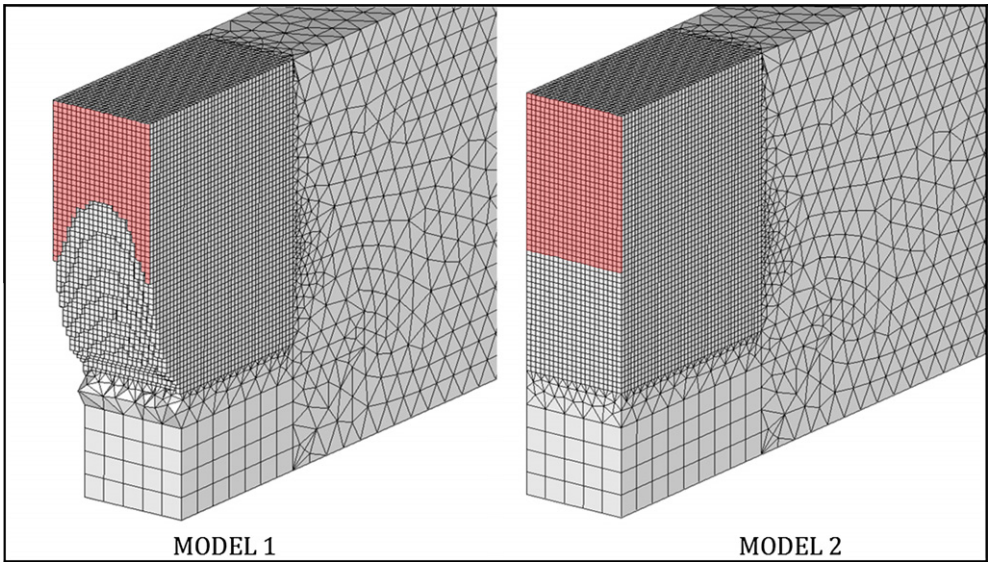

Fig. 10. Finite element meshes for MODEL 1 and MODEL 2.

Please cite this article in press as: Marotta E et al. Effect of fracture tunneling in DWT Tests. Engng Fract Mech (2011), doi:10.1016/j.engfracmech.2011.09.003

5. Effect of inner crack profile on r^* determination

It is now clear that the fracture tunneling develops in the thickness in a three dimensional shape. Although, the kinematic models [8,12] all accounts of a 2-D fracture propagation. In practice, they average the tunneling on a unique front. This simplification can be still adopted, but the interesting point is if one can find an equivalent position of the fracture, able to match the 3-D solution.

To this goal, two 3-D FE models have been developed (Fig. 10). In the first one (MODEL 1), all of the mesh elements inside the tunneling volume were deleted. According to the hypothesis of self similarity of the crack during propagation, the element erase is known if one applies the superficial appearance of the crack, as monitored by experiments. The second mesh (MODEL 2) is the simple extrusion of the 2-D representation where the crack tip position is given by surface appearance.

The typical shape of load-hammer displacement and ligament curves are represented in Fig. 11. The reference condition is given by the residual ligament equal to 30 mm. To this condition corresponds the imposed displacement, the fracture surface position and the applied load. The comparison between FEM and experiments is performed in this condition.

The first comparison (Table 2), shows the excellent overlapping of the experimental condition and the results given by MODEL 1. In synthesis, by imposing the same displacement it returns a very close applied load. On the contrary, the results performed by MODEL 2 considerably deviates from experiments.

If one pretends to apply the 2-D kinematic models given in [8,12], it is necessary to get an equivalent tip location from the point of view of specimen compliance. Subsequent MODELS 2*a*–*h* are similar to previous MODEL 2 but the fracture head is moved towards the inner tip location of the 3-D model. The compliance results show that an excellent agreement can be found for MODEL 2*d*. Here the crack tip is intermediate between the location measured on the surface and the inner tip. This is not the only point of interest. The second one regards an important parameter used in DWTT data interpretation. This parameter is called r^* [27] and reflects the instantaneous center of curvature of the two specimen halves during relative

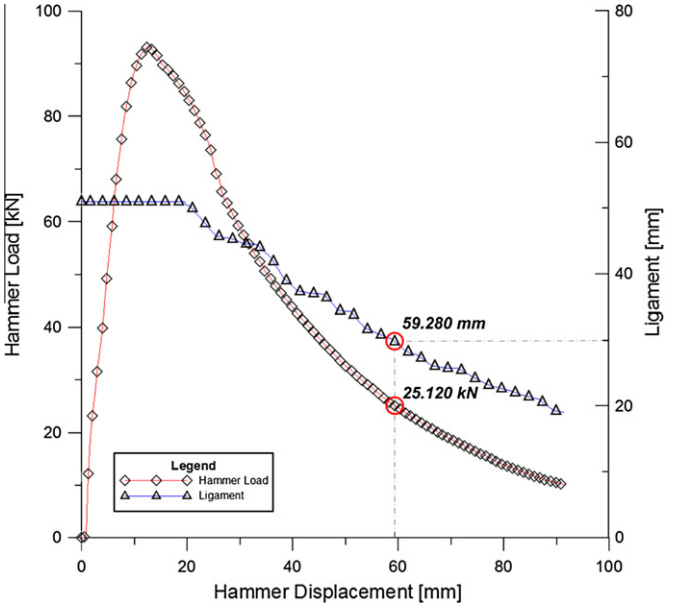

Fig. 11. Hammer load–displacement and ligament curves of X100 test.

Table 2
Comparison among different Finite element MODEL results.

Model	Load (kN)	Tip position (mm)	r^*	$r^*_{effective}$
1	22,374	47–60	0.6606	0.5313
2	42,098	47	0.3103	0.5005
2*a*	27,638	53	0.5967	0.4431
2*b*	25,524	54	0.6131	0.4657
2*c*	23,472	55	0.6294	0.4882
2*d*	21,520	56	0.6453	0.5102
2*e*	19,644	57	0.6620	0.5332
2*f*	17,808	58	0.6778	0.5550
2*g*	16,088	59	0.6943	0.5778
2*h*	14,443	60	0.7106	0.6004

Please cite this article in press as: Marotta E et al. Effect of fracture tunneling in DWT Tests. Engng Fract Mech (2011), doi:10.1016/j.engfracmech.2011.09.003

motion, by respect to residual ligament. If one calculates the r^* taking into account of the surface location, very high values result for X100 when compared to those given by less high strength steels. But if one computes the same parameter considering the effective crack location (MODEL 2*d*), the r^* value falls inside the same range experienced with nonhigh strength steels. This means that the tunneling is one important reason for the shift of r^*, discussed in the previous section.

Even simply adopting MODEL 2, considering the effective position of the crack tip (2*d*), it is very interesting to show that the CIR measured during an infinitesimal unloading of the specimen again indicates the solution *2d* as the best representative of the 3-D model.

The final interpretation of all this results is that one can still adopt the 2-D model, thus taking advantage of the simplified kinematic model of the DWTT, but only after an optimal positioning of the crack tip, ahead its surface appearance, thus accounting of the measured tunneling.

6. Conclusion

The influence of crack tunneling in DWT Test used to introduce criteria for crack propagation is discussed. All the methods, generally adopted, make use of the energy dissipated during crack advance. In this context, the effective crack tunneling can modify significantly the results, as shown in the paper. A method to get an economical measurement of the crack tunneling is presented. The method is applied to provide a more realistic modeling of the DWT Test through finite element analysis. The results by FEM agree significantly with the experiments and suggested to consider the effective equivalent crack position in accordance with the numerical results. This equivalent position allows to tune the classical kinematic methods in a more reliable way, as can be seen by the r^* parameter of high strength steels that approaches the values encountered for more traditional steels.

Note that the results refer to quasi-static tests. It is clear that fracture tunneling under dynamic conditions may change, but the method here presented and discussed could be extended to dynamic tests too.

References

[1] Takeuchi I, Makino H, Okaguchi S, Takahashi N, Yamamoto A. Crack arrestability of high-pressure gas pipelines by X100 or X120. In: 23rd World gas conference: Amsterdam; 2006.
[2] O'Donoghue PE, Kanninen MF, Leung CP, Demofonti G, Venzi S. The development and validation of a dynamic fracture propagation model for gas transmission pipelines. Int J Pres Ves Pip 1997;70(1):11–25.
[3] Bonomo F, et al. Survey and tentative revisal of ductile fracture arrest prevision criteria in pipelines for gas transmission. In: Sih GC, Mirabile M. editors. Proc int conf on analytical and experimental fracture mechanics, vol. 1. Sijthoff & Noordhoff – Rome; 1980. p. 553–66.
[4] Schwalbe KH, Newman Jr JC, Shannon Jr JL. Fracture mechanics testing on specimens with low constraint–standardization activities within ISO and ASTM. Engng Fract Mech 2005;72:557–76.
[5] Di Biagio M, Fonzo A, Salvini P. Fracture propagation in DWT back slotted specimens. Int J Fract 2004;128:159–69.
[6] Buzzichelli G, Demofonti G, Venzi S, Kanninen MF. Step by step procedure for the two specimen CTOA test. In: Proc of the 2nd int conf on pipeline technology: Ostend; 1995.
[7] Priest A, Holmes B. A multi-test piece approach to the fracture characterization of linepipe steels. Int J Fract 1981;17(3):277–99.
[8] Xu S, Bouchard R, Tyson WR. Simplified single-specimen method for evaluating CTOA. Engng Fract Mech 2007;74(15):2459–64.
[9] Berardo G, Salvini P, Mannucci G, Demofonti G. On longitudinal propagation of a ductile fracture in a gas line pipe: numerical and experimental analysis. In: International pipeline conference IPC2000: Calgary; October 2000.
[10] Newman JC, James MA, Zerbst U. A review of the CTOD/CTOA fracture criterion. Engng Fract Mech 2003;70:371–85.
[11] James MA, Newman Jr JC. The effect of crack tunneling on crack growth: experiments and CTOA analyses. Engng Fract Mech 2003;70:457–68.
[12] Martinelli A, Venzi S. Tearing modulus, J-integral, CTOA and crack profile shape obtained from the load–displacement curve. Engng Fract Mech 1996;53(2):263–77.
[13] Mahmoud S, Lease K. The effect of specimen thickness on the experimental characterization of critical crack-tip-opening angle in 2024-T351 aluminum alloy. Engng Fract Mech 2003;70:443–56.
[14] Xu S, Tyson WR, Eagleson R. Measurement of CTOA of pipe steels using MDCB and DWTT specimens. In: International pipeline conference IPC2010: Calgary; October 2010.
[15] Marotta E, Minotti M, Salvini P. Utilizzo di immagini digitali per la meccanica della frattura. XXXVIII Convegno AIAS: Torino; September 2009.
[16] Minotti M, Salvini P. New experimental set-up to approach pipeline fracture behavior by three point bending specimens. Fatigue Fract Engng Mater Struct 2011 [under review process].
[17] Martinelli A, Venzi S. Dependence of J tearing modulus, CTOA, and total fracture energy on specimen dimension. Engng Fract Mech 2001;68(14):1575–90.
[18] Fonzo A, Salvini P, Di Biagio M. The no-dimensional plasticity rotational parameter used in DWT Tests: evaluation by means of finite element. Atti XVII Convegno Nazionale IGF17: Bologna; 2004.
[19] Berardo G, Salvini P, Mannucci G, Demofonti G. On longitudinal propagation of a ductile fracture in a gas line pipe: numerical and experimental analysis. In: International pipeline conference IPC2000: Calgary; October 2000.
[20] Matsoukas G, Cotterell B, Mai YW. On the plastic rotation constant used in standard COD tests. Int J Fract 1984;26:49–53.
[21] Wilkowski G, Shim DJ, Brust F, Rudland D, Duan D. Evaluation of fracture speed on ductile fracture resistance. In: Pipeline technology conference: Oostende; October 2009.
[22] Minotti M, Salvini P. Deep fracture profile effect on DWT test for pipeline characterization. In: Pipeline technology conference: Hannover; April, 2011.
[23] Salvini P, Fonzo A, Mannucci G. Identification of CTOA and fracture process parameters by drop weight test and finite element simulation. Engng Fract Mech 2002:2 [Special CTOA Issue].
[24] Pussegoda LN, Verbit S, Dinovitzer A, Tyson W, Glover A, Collins L, et al. Review of CTOA as a measure of ductile fracture toughness. In: International pipeline conference, vol. 1; 2002. p. 247–54.
[25] Vàrady T, Martin RR, Coxt J. Reverse engineering geometric models-an introduction. Comput-Aided Des 1997;29(4):255–68.
[26] Torres J, Menéndez JM. A Practical algorithm to correct geometrical distortion of image acquisition cameras. In: International conference on image processing: Singapore; 2004.
[27] ASTM E436. Standard Test Method for Drop-Weight Tear Tests of Ferritic Steels. 03; 2008.

Please cite this article in press as: Marotta E et al. Effect of fracture tunneling in DWT Tests. Engng Fract Mech (2011), doi:10.1016/j.engfracmech.2011.09.003